ChemPubSoc Europe

DOI: 10.1002/cplu.201800346

CHEMPLUSCHEM Full Papers

SPECIAL ISSUE

Oxacycle-Fused [1]Benzothieno[3,2-*b*][1]benzothiophene Derivatives: Synthesis, Electronic Structure, Electrochemical Properties, Ionisation Potential, and Crystal Structure

Meera Mohankumar,*[a] Basab Chattopadhyay,[a] Rachid Hadji,[b] Lionel Sanguinet,[b] Alan R. Kennedy,[c] Vincent Lemaur,[d] Jérôme Cornil,[d] Oliver Fenwick,[e] Paolo Samorì,[e] and Yves Geerts[a]

The molecular properties of [1]benzothieno[3,2-*b*][1]benzothiophene (BTBT) are vulnerable to structural modifications, which in turn are determined by the functionalization of the backbone. Hence versatile synthetic strategies are needed to discover the properties of this molecule. To address this, we have attempted heteroatom (oxygen) functionalization of BTBT by a concise and easily scalable synthesis. Fourfold hydroxy-substituted BTBT is the key intermediate, from which the compounds 2,3,7,8-bis(ethylenedioxy)-[1]benzothieno[3,2-*b*][1]benzothiophene and 2,3,7,8-bis(methylenedioxy)-[1]benzothieno[3,2-*b*][1]benzothiophene are synthesized. The difference in ether functionalities on the BTBT scaffold influences the ionisation potential values substantially. The crystal structure reveals the transformation of the herringbone motif in bare BTBT towards π-stacked columns in the newly synthesized derivatives. The results are further justified by the simulated HOMO levels of the model compound.

Introduction

Thienoacenes have been attracting interest due to their potential application in materials science, especially in search for high performing organic field effect transistors (OFETs).[1] Among the plethora of such organic semiconductors, [1]benzothieno[3,2-*b*][1]benzothiophene (referred later as BTBT and shown as **1** in Figure 1) derivatives have become the state of the art material for OFETs, attributed by their easily accessible synthetic protocols, exceptional chemical as well as thermal stability, high carrier mobility and modulation of their electronic properties by band gap tuning *via* straightforward functionalization of the core.[2]

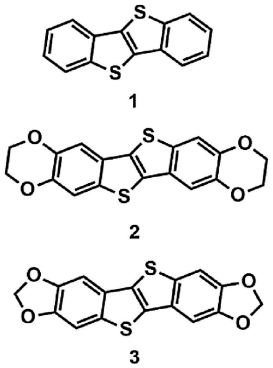

Figure 1. BTBT 1, ether-appended BTBT derivatives 2 and 3.

Even subtle structural variations may lead to unusual changes in their properties; for example, bromination of the BTBT core alters the solid state packing which in turn affects the molecular orbitals' spacing.[3] Therefore, synthetic exploration is essential to gain insight onto the molecular orbitals, redox potentials, π-π stacking and crystal structure.

The basic scaffold of BTBT has been synthesized even on gram scales and easily accessible one step methodologies have also been reported.[4] However, the synthetic efforts have been majorly focussed on the substitution with long alkyl groups at 2,7 positions of the BTBTs owing to their excellent mobility values along with intact solid state ordering facilitated by intermolecular van der Waals interactions of the alkyl groups.[5] On the other hand, introduction of bulky fragments at the same positions have been attempted to gain control over supramolecular organisation.[6] The functionalisation on other

[a] *Dr. M. Mohankumar, Dr. B. Chattopadhyay, Prof. Y. Geerts*
Laboratoire de Chimie des Polymères
Faculté des Sciences
Université Libre de Bruxelles (ULB), CP 206/1
Boulevard du Triomphe, 1050 Bruxelles (Belgium)
E-mail: meerams87@gmail.com
[b] *Dr. R. Hadji, Dr. L. Sanguinet*
LUNAM Université
MOLTECH-Anjou UMRCNRS 6200
Université d'Angers
2 Bd Lavoisier, 49045 Angers Cedex (France)
[c] *Dr. A. R. Kennedy*
Department of Pure and Applied Chemistry
University of Strathclyde
295 Cathedral Street, Glasgow G1 1XL (Scotland, UK)
[d] *Dr. V. Lemaur, Prof. J. Cornil*
Service de Chimie des Matériaux Nouveaux
Université de Mons (UMons)
Place du Parc 20, 7000 Mons (Belgium)
[e] *Dr. O. Fenwick, Prof. P. Samorì*
Université de Strasbourg
CNRS, ISIS
8 alleé Gaspard Monge, 67000 Strasbourg (France)

Supporting information for this article is available on the WWW under https://doi.org/10.1002/cplu.201800346

This article is part of a Special Issue on "π-Conjugated (Macro)molecules and their Applications".

positions of BTBT core is relatively less explored[7] although such molecules are prophetic in patents.[8] The reason behind this might be the tedious synthetic pathways as well as the lack of modular building blocks.

Alternately, computational predictions emphasize heteroatom functionalisation of the organic semiconductor core as an efficient pathway in comparison to extension of π conjugated systems in yielding stable and efficient organic semiconductors.[9] This perception has triggered various synthetic advances towards heteroatom containing organic semiconductors,[10] however such modification is rare on BTBT core.[11] In this context we became interested in particularly oxygen containing BTBT ethers, that are expected to have lower oxidation potential which is pertinent in carrier injection aspects of OFETs.[12] Among ether functionalized acenes, oxacyclic ethers are preferred over alkyl analogues due to their stability and possibility of better ordering in the solid state.[13] In a recent report by Mori *et al.*, the synthesis of dihydroxy BTBT is provided which is further used as a hydrogen bonding motif for studying the solid state arrangement in its charge transfer salt.[14] This intermediate fuelled our interest in designing the fourfold oxy-functionalised BTBTs to explore the molecular properties focusing on the influence of oxygen atom on the structural orientation.

Herein, we report a simple, inexpensive and straightforward synthetic strategy to afford the tetrahydroxy BTBT which is a highly relevant intermediate towards variously functionalised BTBT systems. As a preliminary study, the synthesis of two new oxacyclic BTBTs 2,3,7,8-bis(ethylenedioxy)-[1]benzothieno[3,2-*b*][1]benzothiophene (**2**) and 2,3,7,8-bis(methylenedioxy)-[1]benzothieno[3,2-*b*][1]benzothiophene (**3**) are depicted along with their electrochemical, electronic, and single crystal structure which are compared to the well documented BTBT. To the best of our knowledge this is the first time the depicted strategy has been utilised on BTBT for fourfold functionalization. Our synthetic protocol can be considered as a promising starting point, as the tetrahydroxy BTBT appears to be a prolific intermediate towards a number of interesting chemical transformations on the BTBT core.

Results and Discussion

For the synthesis of oxacyclic BTBT, the attachment of the heteroatom to the core was achieved *apriori* (Scheme 1). Starting from 6-bromo veratraldehyde **4**, acetal protection of the aldehyde functionality was effected with trimethyl orthoformate in quantitative yield. Then Br/Li exchange on **5** was carried out in THF at −78 °C which was followed by S-methylation resulting in 4,5-dimethoxy-2-(methylthio)benzaldehyde **6**. McMurry coupling on **6** resulted in desired stillbene **7** in 65% yield. The cyclisation was effected on the stillbene by treating with excess of I_2 in refluxing acetic acid[7] under dark, to result in the 2,3,7,8-tetramethoxy BTBT **8** in 87% yield. **8** was used as the parent compound on which four fold deprotection of the methoxy groups were carried out using an excess of BBr_3 (8 equiv.) resulting in the 2,3,7,8-tetra hydroxy BTBT **9** in 95%

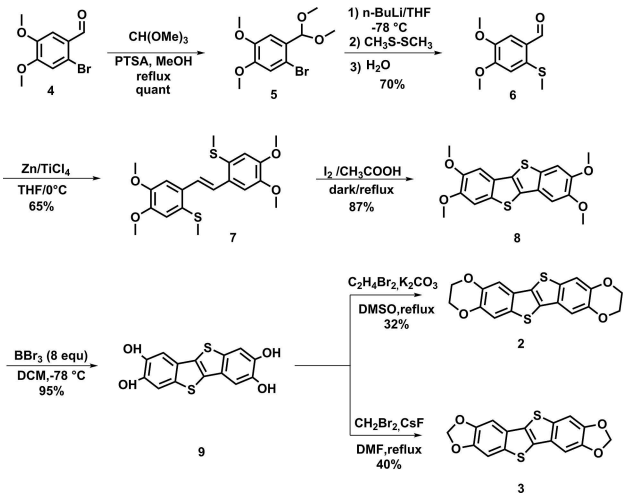

Scheme 1. Synthesis of 2,3,7,8-bis(ethylenedioxy)-[1]benzothieno[3,2-*b*][1]benzothiophene (**2**) and 2,3,7,8-bis(methylenedioxy)-[1]benzothieno[3,2-*b*][1]benzothiophene (**3**).

yield. This molecule being particularly reactive was used in the next step immediately. Compound **9** was subjected to alkylation using 1,2 dibromoethane in DMSO[13b] resulting in dioxane fused BTBT **2** which was purified by vacuum sublimation. O-Alkylation of **9** by adapting a modified protocol[15] using CsF and dibromomethane in DMF was attempted to synthesize **3** in 40% yield (after vacuum sublimation). Starting from compound **4**, the overall yield of **2** and **3** were 12% and 15% respectively. The synthesized BTBT derivatives possess reasonable solubility in common organic solvents and were fully characterized by NMR, mass spectrometry, UV/Vis spectroscopy, and cyclic voltammetry (Refer the **ESI**).

As already reported, substituted and unsubstituted BTBT derivatives are known to present at least one oxidation process which conducts to the corresponding radical cation species. In this context, electrochemical behaviour of the BTBT core is strongly affected by changing the nature and the position of the substituents. For this reason, the electrochemical properties of the 2,3,7,8-tetramethoxyBTBT **8** was investigated, in dichloromethane, by cyclic voltammetry (CV) (Figure S19). Electronically, **8** resembles to the target compounds **2** and **3** but it has the decisive advantages to be considerably more soluble and to be accessible in larger amount. Methoxy groups introduced onto the molecular backbone in any position may simply act as an electron-donating group. As expected, compound **8** shows two successive oxidation processes at 0.55 and 1.10 V (vs Fc^+/Fc) which could be reasonably assigned to the formation of the corresponding radical cation and the dication species respectively. More surprisingly, the stability of the isolated radical is only observed at high scan rate (5 $V s^{-1}$) that is translated on the CV by a perfect reversibility of the signal. In fact, at lower scan rate, the reduction peak presents all characteristics of adsorption phenomenon including a cathodic shift of the potential (even when the platinum electrode is replaced by a vitreous carbon one). The appearance of any new signal in oxidation during subsequent cycles allows us to suggest that

the radical cation is not involved in any polymerisation process but more probably in intramolecular pi-stacking as already observed for rich planar electron donor such as tetrathiafulvalene.[16] Ionisation potentials (IP) of powders of compounds **2** and **3** have been measured by photoelectron spectroscopy in air (PESA). Surprisingly, IP differs substantially. **2** affords a value of 5.7 eV whereas **3** exhibits a much lower ionisation potential of 5.2 eV (Figures S20 and S21). The results are in the same range as previous measurements on other BTBT derivatives, which highlight once more the large importance that crystal packing has on optoelectronic properties.[17,18] The properties of the newly synthesized compounds are listed in Table 1.

Table 1. Optoelectronic properties of BTBTs 8, 2 and 3.

	Exptl. IP [eV]	Predicted HOMO [eV]	Predicted LUMO [eV]	Optical band gap [eV][b]	λmax [nm][c]
8	–[a]	−4.92	−0.8	3.553	344
2	5.7	–	–	3.532	347
3	5.2	–	–	3.512	350

[a] Not measured. [b] Calculated from the absorption edge using Tauc plot. [c] Solution absorption spectra in DMSO.

Single crystals of **2** were grown from hot DMSO while those of **3** were obtained by solubilizing the compound in melted naphthalene followed by slow cooling. Molecular views of the compounds **2** and **3** are given in Figure 2. Both the compounds

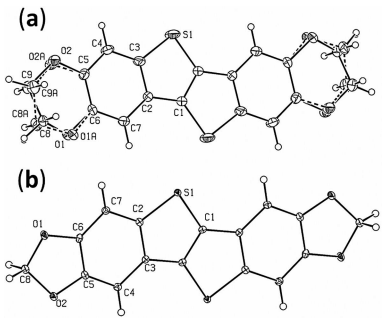

Figure 2. Molecular view of compounds **2** (a) and **3** (b), showing the atom-labelling scheme. Displacement ellipsoids are drawn at the 30% probability level. Unlabelled atoms are generated by symmetry. A detailed crystal data table is given in Table S1 in the Supporting information.

crystallize in a monoclinic unit cell with Z' = 0.5, that is the asymmetric unit contains half of each molecule. The space group of compound **2** is P21/n while for **3** it is C2/c. The crystal structures of the compounds **2** and **3** are shown in Figure 3.

The crystal structures in both **2** and **3** are mainly stabilized by C–H···O type hydrogen bonds coupled with π···π interactions while in **2** C–H···π interactions also contributes to the overall crystal packing. The unsubstituted BTBT **1** crystallises in a "layer by layer" organization where molecules in each layer are packed

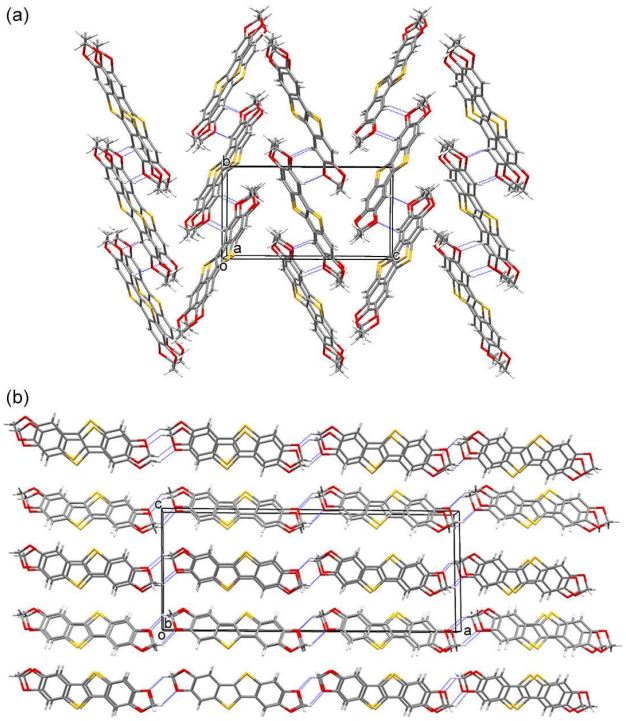

Figure 3. (a) Crystal packing diagram for compound **2**; C–H···O bonds are shown with dotted lines while the stacked molecules interact *via* π···π interactions. (b) Crystal packing diagram for compound **3**; C–H···O bonds are shown with dotted lines while the stacked molecules interact *via* π···π interactions leading to a parallel two-dimensional network in the crystallographic b-direction.

in a herringbone arrangement[19] which is a very common packing motif observed in other BTBT derivatives.[5a],[6a],[17] However, the crystal structure in compounds **2** and **3** is stabilized by π···π interactions forming parallel cofacial π-stacked columns. Such coplanar crystal packing have been observed in brominated BTBT[3] as well as in other thieno[3,2-*b*] thiophene derivatives like BBTBDT.[20] As observed in compound **2** (Figure 3a), each π-stacked column is bound to its nearest neighbour by C7-H7···O1 type bonds forming a 2-dimensional network. C–H···π interactions only act as additional reinforcement within these 2-dimensional assemblies in **2**. In compound **3**, C8-H8 A···O1 H-bond connects adjacent molecules to form parallel H-bonded steps. Further the intermolecular π···π interactions connect the parallel steps in form of two dimensional sheets (Figure 3b). Interestingly, similar dioxolane-functionalized pentacenes have shown to form herringbone structure as well as "rolled" π-stack assembly depending on the nature of the substitution.[13c] These results reaffirm the fact that similar kinds of structural modification on organic semiconductor cores cannot be generalized.

In order to have a clear quantitative and visual insight into the intermolecular interactions, the Hirshfeld surfaces of unsubstituted BTBT **1**, compounds **2** and **3**, and brominated BTBT are illustrated in Figure S22, showing surfaces that have been mapped over a d_{norm} range of −0.15 to 1.50 Å. This allows a rational understanding of the subtleties of crystal packing arising due to BTBT functionalization. The dominant intermo-

lecular interactions in the Hirshfeld surfaces can be observed as the bright red spots which are essentially a manifestation of the C–H···O interactions in **2** and **3** while they correspond to C–H···π interactions in **1** and H···Br contacts in Br-BTBT-Br. Analysis of the 2D fingerprint plots (Figure 4) clearly reveals the differences

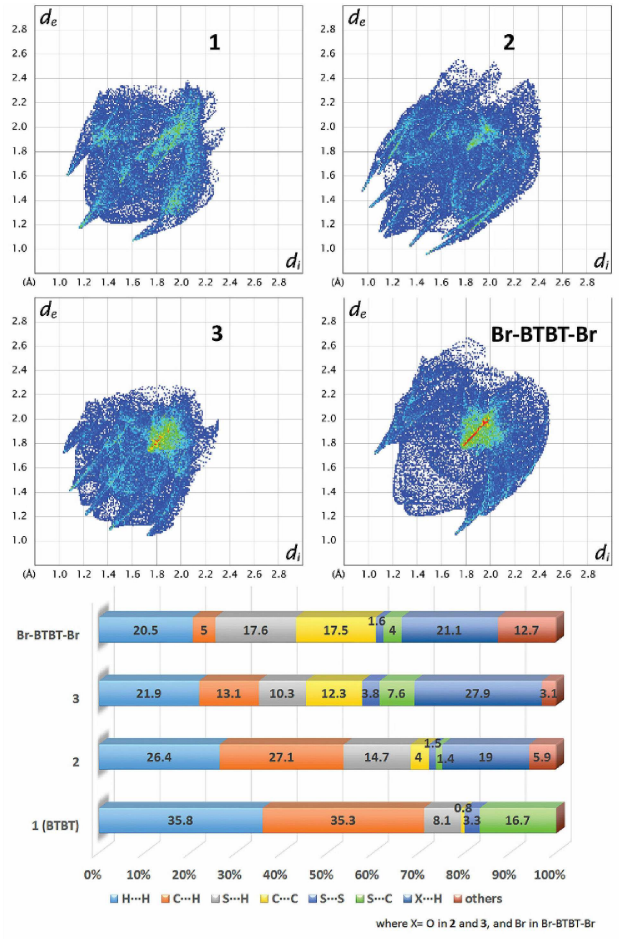

Figure 4. Top panels: Fingerprint plots for compounds **1**, **2**, **3** and Br-BTBT-Br. Bottom panel: Relative contributions to the Hirshfeld surface areas for the various intermolecular contacts for compounds **1**, **2**, **3** and Br-BTBT-Br.

in the packing environments of all the compounds. The C–H···π bonds in **1** and **2** are well manifested and appear as a pair of spikes of almost equal lengths around the (di, de) regions (1.6 Å, 1.1 Å) and (1.1 Å, 1.6 Å). In both **2** and **3**, presence of spikes in the (di, de) regions (1.4 Å, 1.1 Å) and (1.1 Å, 1.4 Å) are due to the presence of C–H···O bonds. In case of **3** and Br-BTBT-Br, the pair of wings appearing at (di, de) regions of (1.7 Å, 1.1 Å) and (1.1 Å, 1.7 Å) are a manifestation of short S···H contacts. The presence of high concentration of points around the regions di = de = 1.8 Å in **3** and Br-BTBT-Br suggests the higher contribution of π···π interactions to the crystal packing in these two compounds. In Br-BTBT-Br the contribution of Br···Br contacts can also be traced in di = de regions spanning from 1.8–2.0 Å. The relative area are depicted in Figure 4 (bottom panel) for all the compounds. In **2** and **3** C–H···O interactions play the major role in the overall crystal packing. The contribution of O···H contacts to the Hirshfeld surface is 19% in **2** and 27.9% in **3**. The quantitative analysis shows that C···H contacts corresponding to C–H···π interactions account for 35.3% in **1** and 27.1% in **2** while in **3** and Br-BTBT-Br it is respectively 13.1% and 5% of the Hirshfeld surface area. In Br-BTBT-Br where the packing is mainly governed by π···π interactions the contribution of C···C contacts is significantly higher at 17.5% while in **1** it is only 0.8%. The S···H contacts also vary significantly, from 8.1% in **1** to 17.6% in Br-BTBT-Br.

Finally, the geometric and electronic properties of isolated tetramethoxy-substituted BTBT **8** have been investigated at the quantum-chemical level (Density Functional Theory — B3LYP/6-31G**). It exhibits two stable conformers, with the most stable planar (Figure 5) and the second less stable by about 4.5 kcal/

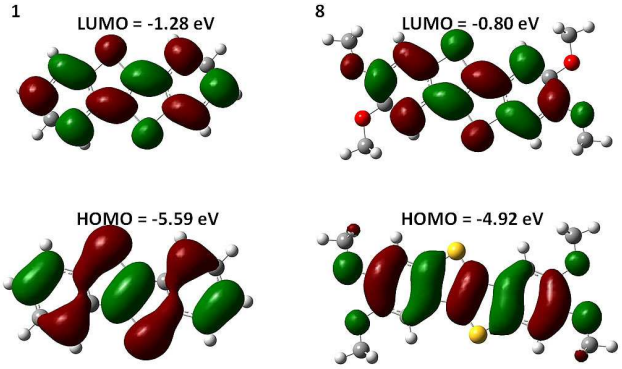

Figure 5. Representation of the shape of the HOMO and LUMO levels of unsubstituted BTBT **1** (left) and tetramethoxy-substituted BTBT **8** (right).

mol that exhibits methyl groups being perpendicular to the molecular plane (Figure S23).

The highest occupied molecular orbital (HOMO) of **8** is destabilized by 0.67 eV compared to the unsubstituted BTBT (−4.92 eV and −5.59 eV for **8** and **1**, respectively), which should impact hole injection from electrodes. The shape of the HOMO wavefunction is also significantly modified by the methoxy substitution leading to the appearance of nodes on the sulfur atoms. Interestingly, this new orbital pattern originates from the increase in the conjugation pathway over the oxygen atoms; as a matter of fact, when the methyl groups lie perpendicular to the conjugated backbone, oxygen atoms are less coupled to the π-electrons of the BTBT core and the HOMO wavefunction resembles that of an unsubstituted BTBT (Figure S23). Since compounds **2** and **3** are planar in their crystalline structure, the ether substitution is expected to modify the shape of the HOMO level and hence their hole transport properties. However, quantifying this impact is quite difficult on the basis of single molecule properties since it requires a combined quantum-chemical and kinetic Monte Carlo study[6,17–19] which is out of the scope of the present paper.

Recently, several reputed scientists have warned the organic electronic community that non-optimized OFETs are dominated by electrical contact resistance that give rise to overestimated mobility values.[27] Since a comprehensive electrical character-

ization with reliable transport properties is out of the scope of this manuscript, we prefer not to report unreliable mobility values from quickly fabricated OFETs.

Conclusion

Two new oxacycle-fused BTBT derivatives have been designed and synthesised successfully to evaluate the effect of such functionalization on the molecular electronic properties and crystal packing. When two oxygen atoms are incorporated in the BTBT core in six-membered and five-membered rings, the shape of the HOMO is significantly modified with no more weight on the sulfur atoms. The packing in the solid state changes also from a herringbone motif to parallel cofacial π-stacked columns. These results show that very subtle synthetic modifications can evoke interesting changes in orbital geometry and in the solid-state ordering which eventually determines all the characteristic molecular and optoelectronic properties.

Experimental Section

Chemicals

All chemicals were purchased from Aldrich or Acros and used without further purification unless stated otherwise. All reactions using n-BuLi were performed in oven-dried glassware under Ar atmosphere. THF was dried by distillation over Na in the presence of benzophenone. Anhydrous *N*, *N*-dimethylformamide was kept over 4 Å molecular sieves. Column chromatography: SiO_2 Kieselgel 60 (Macherey-Nagel, particle size 0.04–0.063 mm). TLC: precoated SiO_2 plates Kieselgel 60F254 (Merck). ^{1}H-NMR (300 MHz) and ^{13}C-NMR (75 MHz) spectra were recorded on a Bruker Avance 300 spectrometer; chemical shifts (δ) are given in ppm and the coupling constants (*J*) in Hz. The residual signal of the solvent was taken as internal reference standard. Electron impact mass spectra (EI-MS) were recorded on a Waters AutoSpec 6F instrument.

1-Bromo-2-(dimethoxymethyl)-4,5-dimethoxybenzene 5: A mixture of 2-bromo-4,5-dimethoxybenzaldehyde (12.5 g, 51 mmol), trimethyl-O-formate (6.5 g, 61.2 mmol) and p-toluenesulfonic acid (97 mg, 0.51 mmol) in methanol (75 mL) was refluxed under argon for 16 h. After cooling to room temperature, the crude mixture was poured into a saturated solution of $NaHCO_3$.The mixture was extracted with diethyl ether. The combined organic layer was further washed with brine and dried over $MgSO_4$, filtered and evaporated. 30.0 g of **5** was obtained in pure form as yellow oil in quantitative yield which becomes solid on cooling. Spectral data were in agreement with the already reported value.[21]

4,5-Dimethoxy-2-(methylthio)benzaldehyde 6: A 2.5 M solution of n-BuLi in hexanes (49.6 mL, 123.9 mmol) was added slowly to a solution of **5** (30.06 g, 103.29 mmol) in anhydrous THF (500 mL) at −78 °C under argon. After 1 h, a solution of dimethyldisulfide (23 mL, 258.23 mmol) was added dropwise and the resulting mixture was stirred at −78 °C for 3 h and at room temperature for 16 h.The solution was then carefully poured into water (300 mL). The mixture was extracted with CH_2Cl_2 (5×100 mL) and the combined organic layer was further washed with brine, dried over $MgSO_4$, filtered and evaporated. The crude was then purified by washing with hot hexane.15.32 g of **6** was obtained as beige powder in 70% yield.mp 106–111 °C; ^{1}H NMR ($CDCl_3$, 300 MHz):δ 2.49 (s, 3H), 3.92 (s, 3H), 3.97 (s, 3H), 6.90 (s, 1H), 7.37 (s, 1H), 10.37 (s, 1H); ^{13}C NMR ($CDCl_3$, 75 MHz) δ 18.6, 56.2, 56.3, 111.6, 112.0, 128.1, 136.7, 148.1, 154.1, 189.9; EI-HRMS obsd 212.0512, calcd 212.0507 [$C_{10}H_{12}O_3S$].

(E)-1,2-Bis(4,5-dimethoxy-2-(methylthio)phenyl)ethane 7: To a suspension of Zn (4.62 g, 70.66 mmol) in anhydrous THF (200 mL) at 0 °C, $TiCl_4$ (7.8 mL, 70.66 mmol) was added dropwise, and the resulting mixture was heated at reflux for 1 h. After cooling down to 0 °C, a solution of **6** (5 g, 23.55 mmol) in anhydrous THF (50 mL) was added, and the resulting mixture was heated at reflux overnight. After cooling to room temperature, the mixture was poured in saturated solution of $NaHCO_3$ (200 mL) and dichloromethane (200 mL) and stirred for 1 h. The mixture was filtered through celite pad and washed with hot $CHCl_3$, and the layers of the filtrate were separated. The aqueous layer was extracted with dichloromethane, and the combined organic layer was dried over $MgSO_4$, filtered and evaporated. Recrystallization from toluene yielded **7** as yellow solid (3 g, 65%): mp 158–164 °C; ^{1}H NMR ($CDCl_3$, 300 MHz):δ 2.41 (s, 6H), 3.92 (s, 6H), 3.96 (s, 6H), 6.97 (s, 2H), 7.18 (s, 2H), 7.49 (s, 2H); ^{13}C NMR ($CDCl_3$, 75 MHz) δ 19.2, 56.2, 108.9, 114.3, 126.4, 127.9, 131.8, 148.6, 149; EI-HRMS obsd 392.1103, calcd 392.1116 [$C_{20}H_{24}O_4S_2$].

2,3,7,8-Tetramethoxy-[1]benzothieno[3,2-*b*][1]benzothiophene 8: A solution of **7** (700 mg, 1.78 mmol) in AcOH (80 mL) at reflux was treated with powdered iodine (14.5 g, 57.06 mmol) and refluxed for 16 h under argon in dark. After cooling to room temperature, the mixture was poured in sodium bisulphite solution (200 mL), and the solid collected by filtration. The filtered material was further washed with water and then with methanol. The residue was then subjected to column chromatography (silica, hot $CHCl_3$) to afford **8** as grey solid (560 mg, 87%). ^{1}H NMR ($CDCl_3$, 300 MHz): δ 3.98 (s, 6H), 4.01 (s, 6H), 7.22 (s, 2H), 7.33 (s, 2H); ^{13}C NMR ($CDCl_3$, 75 MHz) δ 56.3, 56.4, 103, 105.9, 127, 131.9, 134.1, 148.2, 148.6; EI-HRMS obsd 360.0493, calcd 360.0490 [$C_{18}H_{16}O_4S_2$]. UV-vis abs.: λ_{max} = 344 nm (DMSO)

2,3,7,8-Tetrahydroxy-[1]benzothieno[3,2-*b*][1]benzothiophene 9: A 1 M solution of BBr_3 in DCM (22.2 mL, 22.2 mmol) was added in drops to a solution of **8** (1 g, 2.77 mmol) in anhydrous DCM (50 mL) at −78 °C. The resulting reaction mixture was stirred at −78 °C for 4 h and 12 h at room temperature. The crude mixture was poured into water and the resulting solid was filtered and washed with water and then with DCM. The residue was finally taken in acetone and evaporated to get **9** as brown solid (780 mg, 95%). ^{1}H NMR (DMSO, 300 MHz): δ 7.12(s, 2H), 7.31 (s, 2H), 9.38 (d, J = 18 Hz, 4H); ^{13}C NMR (DMSO, 75 MHz) δ 106.2, 109.6, 125.7, 129.9, 131.8, 145.0, 145.1. EI-HRMS obsd 303.9863, calcd 303.9864 [$C_{14}H_8O_4S_2$].

2,3,7,8-Bis(ethylenedioxy)-[1]benzothieno[3,2-*b*][1]benzothiophene 2: Potassium carbonate (4.25 g, 30.75 mmol) was added to a solution of **9** (780 mg, 2.56 mmol) in anhydrous DMSO (20 mL) and stirred under argon. Then 1, 2-dibromoethane (1.20 g, 6.41 mmol) was added in drops and refluxed for 20 h. After cooling to room temperature the reaction mixture was poured into water and the solid was filtered out which was further subjected to vacuum sublimation (source temperature: 360 °C under ~10^{-5} Pa) to get **2** as yellow solid (290 mg, 32%).^{1}H NMR (DMSO, 400 MHz): δ 4.32 (s, 8H), 7.41 (s, 2H), 7.59 (s, 2H); ^{13}C NMR (DMSO, 100 MHz) δ 64.1, 64.2, 108.3, 111.7, 126.9, 131.1, 134.1, 142.6, 142.7 ; EI-HRMS obsd 356.0185, calcd 356.0177 [$C_{18}H_{12}O_4S_2$]. UV-vis abs.: λ_{max} = 347 nm (DMSO)

2,3,7,8-Bis(methylenedioxy)-[1]benzothieno[3,2-*b*][1]benzothiophene 3: Cesium fluoride (2.5 g, 16.43 mmol) was added to a solution of **9** (500 mg, 1.64 mmol) in anhydrous DMF (5 mL).Once reaction mixture became cooler, added dibromomethane (714 mg,

4.11 mmol) in drops and refluxed under argon for 20 h.After cooling to room temperature the reaction mixture was poured into sodium bisulphite solution and the residue was filtered and washed with saturated solution of K_2CO_3 followed by water and then with methanol. The brownish solid was further subjected to vacuum sublimation (source temperature: 330 °C under ~10^{-5} Pa) to get **3** as yellow powder (215 mg, 40 %).^{1}H NMR (DMSO, 300 MHz): δ 6.13 (s, 4H), 7.52 (s, 2H), 7.67 (s, 2H); EI-HRMS obsd 327.9862, calcd 327.9864 [$C_{16}H_8O_4S_2$]. UV-vis abs.: λ_{max} = 350 nm (DMSO).

Single-Crystal X-ray Diffraction

Single-Crystal data collection was carried out with Oxford Diffraction Xcalibur E using MoKα radiation (λ = 0.71073 Å). The crystal structure was solved by direct methods using SIR92[22] for **2** and SHELXS[23] for **3**. Refinement of the crystal structures was performed by full matrix least-squares methods based on F^2 using SHELXL-2014/7[23] and Sheldrick, G. M. SHELXTL Version 2014/7 [http://shelx.uni-ac.gwdg.de/SHELX/index.php]. In **2** the terminal dioxane group was disordered equally over two orientations. The disordered atoms were treated by using EADP, DELU and SIMU instruction in SHELXL-2014/7. The displacement parameters of all non-H-atoms were treated anisotropically. H-atoms were placed at calculated positions using suitable riding models with fixed isotropic thermal parameters [$U_{iso}(H) = 1.2U_{eqv}(C)$ for CH and CH_2 groups]. Crystal data for **2** and **3** are summarized in Table S1. CCDC 1844503 (**2**) and 1844504 (3) contain the supplementary crystallographic data for this paper. These data are provided free of charge by The Cambridge Crystallographic Data Centre.

Hirshfeld Surface Analysis

Hirshfeld surfaces[24] and the associated fingerprint plots[25] were calculated using Crystal Explorer, [*Crystalexplorer (Version 3.1)*, University of Western Australia: 2012] which accepts a structure input file in the CIF format. Bond lengths to hydrogen atoms were set to typical neutron values (C–H = 1.083 Å). For each point on the Hirshfeld isosurface, two distances d_e, the distance from the point to the nearest nucleus external to the surface, and d_i, the distance to the nearest nucleus internal to the surface, are defined. The normalized contact distance (d_{norm}) based on d_e and d_i is given by Equation (1)

$$d_{norm} = \frac{(d_i - r_i^{vdW})}{r_i^{vdW}} + \frac{(d_e - r_e^{vdw})}{r_e^{vdW}} \quad (1)$$

where r_i^{vdW} and r_e^{vdW} are the van der Waals radii of the atoms. The value of d_{norm} is negative or positive depending if the intermolecular contacts are shorter or longer than the van der Waals separations. The parameter d_{norm} displays a surface with a red-white-blue color scheme, where bright red spots highlight shorter contacts, white areas represent contacts around the van der Waals separation, and blue regions are devoid of close contacts.

Electrochemistry

Dichloromethane (HPLC grade) and tetra-n-butylammonium hexafluorophosphate (TBAP, electrochemical grade, Fluka was recrystallised from ethanol). Cyclic voltammetry (CV) was performed in a three-electrode cell equipped with a platinum milli-electrode, a platinum wire counter-electrode and a silver wire used as a quasi-reference electrode. The electrochemical experiments were carried out under a dry and oxygen-free atmosphere (H_2O < 1 ppm, O_2 < 1 ppm) in CH_2Cl_2 with TBAP (0.1 M) as the support electrolyte. The voltammograms were recorded on a potentiostat/galvanostat (Bio-Logic – SP150) driven by the EC-Lab software with positive feedback compensation. Based on repetitive measurements, absolute errors on potentials were estimated to be ≈ ±5 mV. All the potential reported below, were calibrated versus Ferrocene/Ferrocenium oxidation potential (+0.405 V *vs* SCE or +0.425 V *vs.* Ag/AgCl).

Photoelectron Spectroscopy in Air (PESA)

The ionization potentials of powders of **2** and **3** were measured with an AC-2 Photoelectron Spectrometer (RKI Instruments), working in ambient conditions and scanning the incident UV photon energy from 4.5 eV to 6.2 eV.

Quantum-Chemical Calculations

The geometrical and electronical properties of all the molecules have been calculated within the Gaussian 09 package (Revision A02)[26] at the Density Functional Theory (DFT) level using the B3LYP functional and the 6–31G** basis set.

Acknowledgements

The authors acknowledge support from the Belgian National Fund for Scientific Research (FNRS – PDR T.0058.14). B. C. kindly acknowledges support from the FRS-FNRS (Belgian National Scientific Research Fund) for the POLYGRAD Project 22333186. B. C. is a FRS-FNRS Research Fellow. P.S. acknowledges also the Agence Nationale de la Recherche through the LabEx CSC (ANR-10-LABX-0026_CSC) and the International Center for Frontier Research in Chemistry (icFRC). The work in the Laboratory for Chemistry of Novel Materials was supported by the European Commission/Région Wallonne (FEDER – BIORGEL project), the Interuniversity Attraction Pole program of the Belgian Federal Science Policy Office (PAI 7/05), the Programme d'Excellence de la Région Wallonne (OPTI2MAT project), the Consortium des Équipements de Calcul Intensif (CÉCI), funded by the Fonds de la Recherche Scientifique de Belgique (FRS.-FNRS) under Grant No. 2.5020.11, and FRS-FNRS. J. C. is a FNRS Research Director.

Conflict of Interest

The authors declare no conflict of interest.

Keywords: arenes · crystal engineering · electrochemistry · electronic properties · π-conjugation

[1] a) K. Takimiya, S. Shinamura, I. Osaka, E. Miyazaki, *Adv. Mater.* **2011**, *23*, 4347–4370; b) H. Sirringhaus, *Adv. Mater.* **2014**, *26*, 1319–1335; c) J. H. Gao, R. J. Li, L. Q. Li, Q. Meng, H. Jiang, H. X. Li, W. P. Hu, *Adv. Mater.* **2007**, *19*, 3008–3011; d) R. Li, L. Jiang, Q. Meng, J. Gao, H. Li, Q. Tang, M. He, W. Hu, Y. Liu, D. Zhu, *Adv. Mater.* **2009**, *21*, 4492–4495; e) Y. Miyata, E. Yoshikawa, T. Minari, K. Tsukagoshi, S. Yamaguchi, *J. Mater. Chem.* **2012**, *22*, 7715–7717; f) K. Xiao, Y. Liu, T. Qi, W. Zhang, F. Wang, J. Gao, W. Qiu, Y. Ma, G. Cui, S. Chen, X. Zhan, G. Yu, J. Qin, W. Hu, D. Zhu, *J. Am. Chem. Soc.* **2005**, *127*, 13281–13286; g) K. Takimiya, H. Ebata, K.

Sakamoto, T. Izawa, T. Otsubo, Y. Kunugi, *J. Am. Chem. Soc.* **2006**, *128*, 12604–12605.
[2] K. Takimiya, I. Osaka, T. Mori, M. Nakano, *Acc. Chem. Res.* **2014**, *47*, 1493–1502.
[3] V. S. Vyas, R. Gutzler, J. Nuss, K. Kern, B. V. Lotsch, *CrystEngComm* **2014**, *16*, 7389–7392.
[4] a) S. Haruki, Y. Syuji, *J. Heterocycl. Chem.* **1998**, *35*, 725–726; b) M. Saito, T. Yamamoto, I. Osaka, E. Miyazaki, K. Takimiya, H. Kuwabara, M. Ikeda, *Tetrahedron Lett.* **2010**, *51*, 5277–5280; c) M. Saito, I. Osaka, E. Miyazaki, K. Takimiya, H. Kuwabara, M. Ikeda, *Tetrahedron Lett.* **2011**, *52*, 285–288.
[5] a) H. Ebata, T. Izawa, E. Miyazaki, K. Takimiya, M. Ikeda, H. Kuwabara, T. Yui, *J. Am. Chem. Soc.* **2007**, *129*, 15732–15733; b) C. Liu, T. Minari, X. Lu, A. Kumatani, K. Takimiya, K. Tsukagoshi, *Adv. Mater.* **2011**, *23*, 523–526.
[6] a) G. Schweicher, V. Lemaur, C. Niebel, C. Ruzie, Y. Diao, O. Goto, W. Y. Lee, Y. Kim, J. B. Arlin, J. Karpinska, A. R. Kennedy, S. R. Parkin, Y. Olivier, S. C. Mannsfeld, J. Cornil, Y. H. Geerts, Z. Bao, *Adv. Mater.* **2015**, *27*, 3066–3072; b) H. Iino, T. Usui, J. Hanna, *Nat. Commun.* **2015**, *6*, 6828.
[7] C. Ruzie, J. Karpinska, A. R. Kennedy, Y. H. Geerts, *J. Org. Chem.* **2013**, *78*, 7741–7748.
[8] a) K. Takimiya, H. Kuwahara, T. Yui, M. Ikeda, JP2010001236 A (Hiroshima University, Japan), **2010**; b) A. Wigglesworth, Y. Wu, P. Liu, M. A. Heuft, CA2762471 A1 (Xerox Corporation, USA), **2012**; c) M. Nakatsuka, JP2011258900 A (Yamamoto Chemicals Inc., Japan), **2011**; d) K. Kobayashi, K. Kimura, T. Susuki, H. Satou, Y. Tani, WO2010050575 A1 (FujiFilm Corporation, Japan), **2010**; e) M. Nakatsuka, JP2009021390 A (Yamamoto Chemicals Inc., Japan), **2009**; f) K. Takimiya, S. Shinamura, M. Hamada, Y. Sadamitsu, WO2014030700 A1 (Nippon Kayaku Kabushiki Kaisha, Japan), **2014**.
[9] G. Gryn'ova, C. Corminboeuf, *J. Phys. Chem. Lett.* **2016**, *7*, 5198–5204.
[10] a) L. Yan, Y. Zhao, H. Yu, Z. Hu, Y. He, A. Li, O. Goto, C. Yan, T. Chen, R. Chen, Y.-L. Loo, D. F. Perepichka, H. Meng, W. Huang, *J. Mater. Chem. C* **2016**, *4*, 3517–3522; b) L. Yifan, G. o. Ganna, S. Felipe, J. Xavier, S. Kevin, C. Clémence, W. Jérôme, *Chem. Eur. J.* **2017**, *23*, 8058–8065; c) C. Wang, H. Nakamura, H. Sugino, K. Takimiya, *J. Mater. Chem. C* **2018**, *6*, 3604–3612.
[11] M. Matsumura, A. Muranaka, R. Kurihara, M. Kanai, K. Yoshida, N. Kakusawa, D. Hashizume, M. Uchiyama, S. Yasuike, *Tetrahedron* **2016**, *72*, 8085–8090.
[12] X. Cheng, Y.-Y. Noh, J. Wang, M. Tello, J. Frisch, R.-P. Blum, A. Vollmer, J. P. Rabe, N. Koch, H. Sirringhaus, *Adv. Funct. Mater.* **2009**, *19*, 2407–2415.
[13] a) M. M. Payne, J. H. Delcamp, S. R. Parkin, J. E. Anthony, *Org. Lett.* **2004**, *6*, 1609–1612; b) J. Hellberg, E. Dahlstedt, M. E. Pelcman, *Tetrahedron* **2004**, *60*, 8899–8912; c) J. E. Anthony, J. Gierschner, C. A. Landis, S. R. Parkin, J. B. Sherman, R. C. Bakus Ii, *Chem. Commun.* **2007**, 4746–4748; d) O. L. Griffith, J. E. Anthony, A. G. Jones, Y. Shu, D. L. Lichtenberger, *J. Am. Chem. Soc.* **2012**, *134*, 14185–14194; e) M. J. Bruzek, J. E. Anthony, *Org. Lett.* **2014**, *16*, 3608–3610; f) H. Mori, X. C. Chen, N. H. Chang, S. Hamao, Y. Kubozono, K. Nakajima, Y. Nishihara, *J. Org. Chem.* **2014**, *79*, 4973–4983.
[14] T. Higashino, A. Ueda, J. Yoshida, H. Mori, *Chem. Commun.* **2017**, *53*, 3426–3429.
[15] J. H. Clark, H. L. Holland, J. M. Miller, *Tetrahedron Lett.* **1976**, *17*, 3361–3364.
[16] a) G. Christine, L. Claudia, L. Shi-Xia, S. Lionel, L. Eric, H. Andreas, D. Silvio, *ChemPhysChem* **2007**, *8*, 1504–1512; b) S. Bouguessa, K. Herve, S. Golhen, L. Ouahab, J.-M. Fabre, *New J. Chem.* **2003**, *27*, 560–564.
[17] Y. Tsutsui, G. Schweicher, B. Chattopadhyay, T. Sakurai, J. B. Arlin, C. Ruzie, A. Aliev, A. Ciesielski, S. Colella, A. R. Kennedy, V. Lemaur, Y. Olivier, R. Hadji, L. Sanguinet, F. Castet, S. Osella, D. Dudenko, D. Beljonne, J. Cornil, P. Samori, S. Seki, Y. H. Geerts, *Adv. Mater.* **2016**, *28*, 7106–7114.
[18] C. Ruzie, J. Karpinska, A. Laurent, L. Sanguinet, S. Hunter, T. D. Anthopoulos, V. Lemaur, J. Cornil, A. R. Kennedy, O. Fenwick, P. Samori, G. Schweicher, B. Chattopadhyay, Y. H. Geerts, *J. Mater. Chem. C* **2016**, *4*, 4863–4879.
[19] C. Niebel, Y. Kim, C. Ruzie, J. Karpinska, B. Chattopadhyay, G. Schweicher, A. Richard, V. Lemaur, Y. Olivier, J. Cornil, A. R. Kennedy, Y. Diao, W.-Y. Lee, S. Mannsfeld, Z. Bao, Y. H. Geerts, *J. Mater. Chem. C* **2015**, *3*, 674–685.
[20] T. Yamamoto, T. Nishimura, T. Mori, E. Miyazaki, I. Osaka, K. Takimiya, *Org. Lett.* **2012**, *14*, 4914–4917.
[21] B. A. Keay, H. P. Plaumann, D. Rajapaksa, R. Rodrigo, *Can. J. Chem.* **1983**, *61*, 1987–1995.
[22] A. Altomare, G. Cascarano, C. Giacovazzo, A. Guagliardi, M. C. Burla, G. Polidori, M. Camalli, *J. Appl. Crystallogr.* **1994**, *27*, 435.
[23] G. Sheldrick, *Acta Crystallogr. Sect. A* **2008**, *64*, 112–122.
[24] a) M. A. Spackman, D. Jayatilaka, *CrystEngComm* **2009**, *11*, 19–32; b) A. S. Mark, *Phys. Scr.* **2013**, *87*, 048103.
[25] M. A. Spackman, J. J. McKinnon, *CrystEngComm* **2002**, *4*, 378–392.
[26] M. J. Frisch, Gaussian 09 (Gaussian, Inc., Wallingford CT, **2009**).
[27] a) Y. Chen, B. Lee, H. T. Yi, S. S. Lee, M. M. Payne, S. Pola, C.-H. Kuo, Y.-L. Loo, J. E. Anthony, Y. T. Tao, V. Podzorov, *Phys. Chem. Chem. Phys.* **2012**, *14*, 14142–14151; b) D. Choi, P.-H. Chu, M. McBride, E. Reichmanis, *Chem. Mater.* **2015**, *27*, 4167–4168. c) E. G. Bittle, J. I. Basham, T. N. Jackson, O. D. Jurchescu, D. J. Gundlach, *Nat. Commun.* **2016**, *7*, 10908; d) T. Uemura, C. Rolin, T.-H. Ke, P. Fesenko, J. Genoe, P. Heremans, J. Takeya, *Adv. Mater.* **2016**, 28, 151–155; e) I. McCulloch, A. Salleo, M. Chabinyc, *Science* **2016**, *352*, 1521–1522; f) H. H. Choi, K. Cho, C. D. Frisbie, H. Sirringhaus, V. Podzorov, *Nat. Mater.* **2018**, *17*, 2–7.

Manuscript received: July 4, 2018
Accepted manuscript online: October 2, 2018